

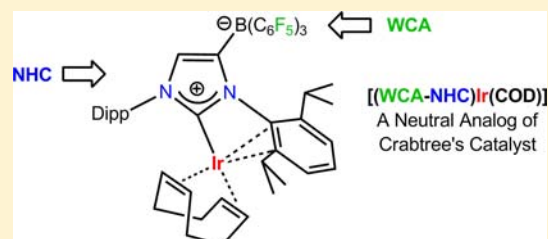
Iridium(I) Complexes with Anionic N-Heterocyclic Carbene Ligands as Catalysts for the Hydrogenation of Alkenes in Nonpolar Media

Eugene L. Kolychev, Sabrina Kronig, Kai Brandhorst, Matthias Freytag, Peter G. Jones, and Matthias Tamm*

Institut für Anorganische und Analytische Chemie, Technische Universität Braunschweig, Hagenring 30, 38106 Braunschweig

S Supporting Information

ABSTRACT: A series of lithium complexes of anionic N-heterocyclic carbenes that contain a weakly coordinating borate moiety (WCA-NHC) was prepared in one step from free N-heterocyclic carbenes by deprotonation with *n*-butyl lithium followed by borane addition. The reaction of the resulting lithium-carbene adducts with $[M(\text{COD})\text{Cl}]_2$ ($M = \text{Rh}, \text{Ir}$; $\text{COD} = 1,5\text{-cyclooctadiene}$) afforded zwitterionic rhodium(I) and iridium(I) complexes of the type $[(\text{WCA-NHC})M(\text{COD})]$, in which the metal atoms exhibit an intramolecular interaction with the N-aryl groups of the carbene ligands. For $M = \text{Rh}$, the neutral complex $[(\text{WCA-NHC})\text{Rh}(\text{CO})_2]$ and the ate complex $(\text{NEt}_4)[(\text{WCA-NHC})\text{Rh}(\text{CO})_2\text{Cl}]$ were prepared, with the latter allowing an assessment of the donor ability of the ligand by IR spectroscopy. The zwitterionic iridium–COD complexes were tested as catalysts for the homogeneous hydrogenation of alkenes, which can be performed in the presence of nonpolar solvents or in the neat alkene substrate. Thereby, the most active complex showed excellent stability and activity in hydrogenation of alkenes at low catalyst loadings (down to 10 ppm).



INTRODUCTION

The seminal reports of Crabtree and co-workers on the catalytic activity of $[\text{Ir}(\text{COD})(\text{py})(\text{PCy}_3)][\text{PF}_6]$ (**A**, “Crabtree’s catalyst”)¹ have directed considerable attention to cationic iridium(I) complexes as active and highly selective hydrogenation catalysts.² Over time, the original structure of **A**, which consists of a cationic square-planar 16-electron Ir(I) complex fragment with an η^4 -coordinated 1,5-cyclooctadiene (COD) and two ancillary ligands (pyridine, py, and tricyclohexyl phosphine, PCy_3) and a PF_6^- counterion, has undergone several modifications to increase its activity, stability, and solubility (Figure 1). Thus, Pfaltz and co-workers introduced chiral catalysts of type **B**, which contain P,N-chelating phosphinoxazolines (PHOX)³ in place of the monodentate PCy_3 and pyridine ligands.⁴ Their use as catalysts for the asymmetric hydrogenation of unfunctionalized olefins was systematically studied, revealing that the catalyst activity and productivity strongly depend on the counterion. Particularly high rates and turnover numbers (TON) were found in the presence of so-called weakly coordinating anions (WCA), such as the BARF ion (Figure 1), allowing a reduction of the catalyst loadings to 0.02 mol %, e.g., for full conversion of (*E*)-1,2-diphenyl-1-propene at room temperature and 14 bar H_2 pressure.^{4b} Further attempts to improve the catalyst performance in nonpolar solvents were made by the groups of Stradiotto⁵ and Pfaltz,⁶ who introduced two different types of zwitterionic⁷ iridium(I) complexes **C** and **D**, in which the anion forms part of the respective chelate ligand. However, **C** showed comparatively low activity in the hydrogenation of styrene in nonpolar media (37% at 0.5 mol % and 1 bar H_2 in benzene

and 17% at 0.5 mol % and 1 bar H_2 in hexanes). In contrast, catalysts of type **D** carrying a covalently bound WCA fragment are able to efficiently catalyze the hydrogenation of trisubstituted alkenes even in hexane (1 mol %, 50 bar H_2), which could not be accomplished with the previous systems.⁸

Another important modification was made by Nolan and co-workers,⁹ who obtained a thermally more stable congener **E** of Crabtree’s catalyst by replacing the phosphine in **A** with an N-heterocyclic carbene (NHC), which can be expected to bind more strongly to the metal atom.¹⁰ In the same year, Burgess and co-workers reported chiral NHC–oxazoline iridium(I) complexes of type **F** for asymmetric hydrogenation of alkenes.¹¹ Since then, a large variety of related phosphine-free NHC¹² and also mixed phosphine–NHC¹³ iridium(I) complexes have been introduced as efficient hydrogenation catalysts.

Recently, we introduced a novel type of anionic N-heterocyclic carbenes with a weakly coordinating borate moiety (WCA-NHC, Figure 1),¹⁴ which was developed as a spin-off from our studies on frustrated carbene–borane Lewis pairs.^{15,16} It was demonstrated that such carbene ligands give access to zwitterionic gold(I) complexes, such as $[(\text{WCA-NHC})\text{Au}(\text{THT})]$ (THT = tetrahydrothiophene), which serve as catalysts for the skeletal rearrangement of enynes even in less polar solvents, such as toluene.¹⁴ Naturally, the coordination of such anionic carbenes to the iridium(I)-cyclooctadiene fragment would potentially add a new member to the large family of Crabtree-type catalysts and combine two of the successful

Received: July 2, 2013

Published: July 24, 2013

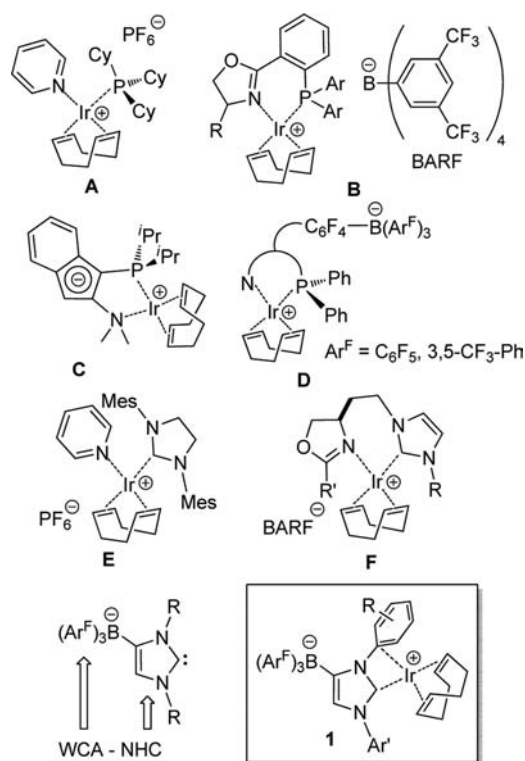


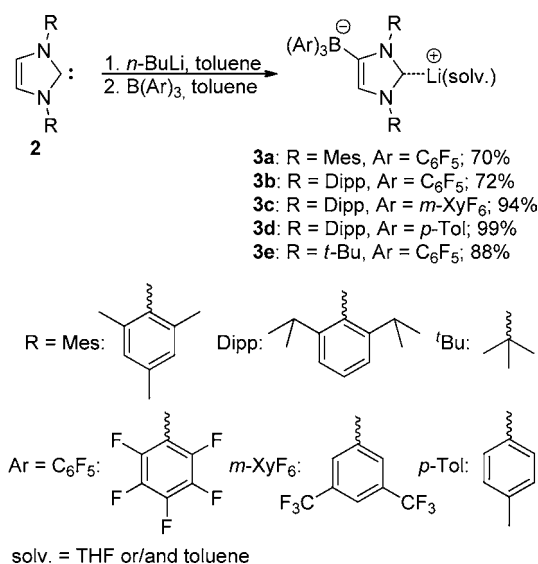
Figure 1. Crabtree's catalyst (A) and modifications thereof; all coordinative bonds are dotted to illustrate the cationic or ylidic nature of the complexes by placing a positive formal charge at Ir and a negative formal charge at the (intramolecular) counterion.

strategies outlined above, i.e., the use of NHC ligands, as present in structures E and F, with that of anionic ligands, as realized in the ylidic structures C and D. Furthermore, the resulting zwitterionic complexes of the type [(WCA-NHC)Ir(COD)] of type 1 might exhibit an intramolecular arene-iridium interaction (Figure 1) and thus afford one-component and neutrally charged catalysts for use in nonpolar solvents. Accordingly, we wish to report herein the synthesis and characterization of iridium(I) complexes of type 1 together with a detailed study of their use as olefin hydrogenation catalysts. In addition, related cyclooctadiene and dicarbonyl rhodium(I) complexes are presented, with the latter serving as a tool to establish the electronic character and donor ability of the new carbene ligands by IR spectroscopy.

RESULTS AND DISCUSSION

Synthesis of Lithium–Carbene Complexes. We have previously reported a two-step procedure for the preparation of the lithium–carbene complexes 3b and 3e.¹⁴ The first step involved deprotonation of the free carbenes 2 with *n*-BuLi in hexane according to the procedure described by Robinson and co-workers.¹⁷ The resulting lithium salts were isolated by filtration and subsequently treated with B(C₆F₅)₃ in toluene solution. We have now modified this procedure to allow for the preparation of the target lithium–carbene complexes as their toluene or THF solvates in one step from the free NHCs (Scheme 1). Accordingly, the respective carbene 2 was deprotonated with *n*-BuLi in toluene, resulting in a jelly-like mass (for R = Dipp) or in suspensions of the deprotonated intermediates, which was followed by addition of the appropriate borane component. Whereas the toluene solvates

Scheme 1. Preparation of the Lithium–Carbene Complexes 3a–3e



3a and 3d could be directly obtained as white powders by filtration, the isolation of 3b, 3c, and 3e required the addition of a few drops of THF to precipitate their THF solvates from toluene solution. This procedure affords the pure complexes 3a–3e in good to excellent yields (70–99%). All lithium complexes are highly air- and moisture-sensitive white solids, which, upon exposure to air, undergo fast hydrolysis and protonation of the carbene carbon atom as demonstrated for 3b. The resulting zwitterionic imidazolium borate was characterized by X-ray diffraction analysis, and its molecular structure (see Supporting Information) is similar to that previously established for the zwitterion formally derived from 3e.^{15a}

The new complexes were characterized by NMR spectroscopy in THF-*d*₈; however, the ¹³C NMR signal of the carbene carbon atom was only detected for 3c at 218.9 ppm, which is upfield from the resonance of the corresponding free carbene IDipp ($\delta = 220.6$ ppm)¹⁸ and close to the chemical shift found for 3b at 217.2 ppm.¹⁴ The introduction of the borate moiety renders the N-substituents magnetically inequivalent, and two different sets of signals are detected for the R groups (Mes, Dipp, *t*-Bu) in the ¹H and ¹³C NMR spectra. Two of the three new lithium complexes were characterized by X-ray diffraction analyses, and selected bond lengths and angles are assembled in Table 1. Complex 3d (Figure 2) has a structure similar to that previously reported for 3b,¹⁴ with the lithium atom residing in a trigonal-planar coordination sphere created by the carbene and two THF ligands (angle sum = 359.9°). The angle between the O1–Li–O2 and N1–C1–N2 planes is 31.3°, which is close to values reported for the lithium complexes of other Dipp-substituted carbene-borates, i.e., 30.4° in 3b and 34.7° in the corresponding Et₃B derivative,^{14,17} whereas an almost perpendicular orientation and therefore significantly larger angle was found for the sterically more congested 3e (81.4°).¹⁴ In contrast, complex 3a, bearing smaller mesityl substituents, displays a four-coordinate lithium atom by binding an additional THF molecule to afford a distorted tetrahedral environment (Figure 3).

Synthesis and Characterization of Rhodium(I) Complexes. To determine the influence of the borate moiety on

Table 1. Selected Bond Lengths [Å] and Angles [°] for Lithium, Rhodium(I), and Iridium(I) NHC Complexes

compound	M	M–C _{carbene}	M–C _{ipso}	M–C _{ortho}	M–C' _{ortho}	M–C1–N1	M–C1–N2	incl. ^a	ref
3a	Li	2.198(2)	3.543(2)	3.975(2)	4.080(2)	129.88(9)	126.77(9)		this work
3b	Li	2.094(3)	3.449(3)	3.860(3)	4.168(3)	130.56(10)	123.53(9)		14
3d	Li	2.100(3)	3.748(3)	3.864(3)	4.088(3)	131.50(11)	126.20(11)		this work
4	Rh	2.027(2)	2.4663(19)	2.6485(23)	3.1378(21)	105.70(14)	149.28(15)	23.5	this work
4 (calcd) ^b	Rh	2.036/2.032	2.609/2.530	2.907/2.727	3.183/3.174	108.7/107.2	145.8/147.0	19.8/22.2	this work
5 ^c	Rh	2.056(4)	3.554(4)	3.910(5)	4.373(5)	128.5(3)	127.2(3)		20
6 (X = BF ₄)	Rh	2.040(4)	2.377(4)	2.624(5)	3.061(4)	101.5(3)	139.7(3)		21a
6 (X = PF ₆) ^c	Rh	2.033(5)	2.353(5)	2.755(6)	2.965(6)	100.7(4)	140.7(4)		21b
7	Rh	2.036(2)	2.346(4)	2.806(2)	2.873(1)	100.93(11)	143.37(12)	23.2	22
8	Rh	2.0133(17)	2.3988(16)	2.5823(17)	2.9862(22)	104.97(11)	149.01(13)		this work
1a	Ir	2.023(3)	2.472(3)	2.706(3)	3.078(2)	105.98(18)	148.5(2)	22.4	this work
1b ^c	Ir	2.027(2)/ 2.026(2)	2.447(2)/ 2.473(2)	2.571(3)/ 2.614(2)	3.146(2)/ 3.163(2)	106.36(16)/ 107.06(16)	148.58(19)/ 147.79(19)	22.4 21.6	this work
1b (calcd) ^b	Ir	2.048/2.044	2.577/2.529	2.876/2.745	3.163/3.161	108.4/107.6	146.0/146.7	20.2/21.8	this work
1c	Ir	2.0242(19)	2.4553(18)	2.7285(20)	3.0411(20)	106.02(13)	148.27(14)	22.3	this work
1d	Ir	2.019(3)	2.487(3)	2.670(3)	3.090(3)	106.90(18)	147.7(2)	21.8	this work

^aInclination defined by $180^\circ - \theta$ with $\theta = \text{M}-\text{C1}-\text{Ct}_{\text{im}}$ (Ct_{im} = centroid of the imidazole ring). ^bValues with the density functionals B3LYP/M06L. The calculated structures of the iridium complexes are shown. ^cValues for one of two independent molecules in the asymmetric unit.

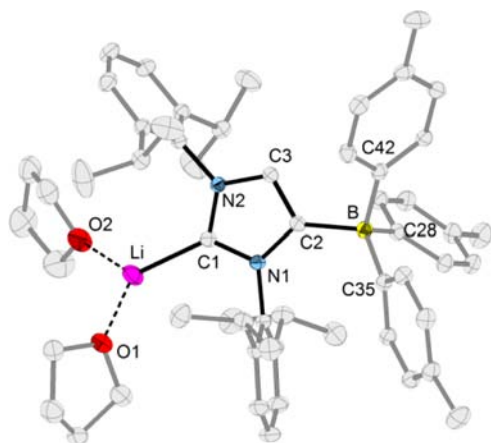


Figure 2. ORTEP diagram of 3d in 3d·2THF with thermal displacement parameters drawn at 30% probability. Hydrogen atoms are omitted for clarity. Selected bond lengths [Å] and angles [°] (see also Table 1): Li–C1 2.100(3), Li–O1 1.894(3), Li–O2 1.917(3), B–C2 1.6548(17); N1–C1–N2 102.14(10), C1–Li–O1 128.69(14), C1–Li–O2 124.12(14), O1–Li–O2 107.09(13).

the donor abilities of the anionic carbene ligands, we aimed at the preparation of rhodium(I) dicarbonyl complexes for assessing the electronic character of the WCA-NHCs by IR spectroscopy.¹⁹ At first, the lithium complex 3b was added to a solution of dimeric $[\text{Rh}(\text{COD})\text{Cl}]_2$ in toluene. After filtration from LiCl, evaporation, and recrystallization from diethyl ether/dichloromethane, the zwitterionic complex 4 was obtained as a yellow crystalline solid in 50% yield (Scheme 2). The ¹H NMR spectrum of 4 exhibits two distinct sets of signals for the CH₂–CH₂ and CH=CH fragments of the COD ligand, which is similar to the situation reported for the complex $[(\text{IDipp})\text{RhCl}(\text{COD})]$ (5) containing the analogous neutral NHC ligand IDipp (Scheme 2).²⁰ Accordingly, the ¹³C NMR spectrum shows two distinct doublets for the metal-bound CH=CH moieties at 101.8 ppm with $^1J(^{13}\text{C}, ^{103}\text{Rh}) = 7.2$ Hz and at 69.2 ppm with $^1J(^{13}\text{C}, ^{103}\text{Rh}) = 17.5$ Hz ppm, with

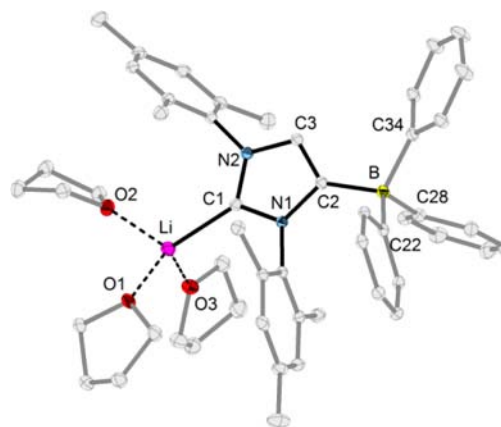


Figure 3. ORTEP diagram of 3a with thermal displacement parameters drawn at 30% probability. Hydrogen and fluorine atoms are omitted for clarity. Selected bond lengths [Å] and angles [°] (see also Table 1): Li–C1 2.198(2), Li–O1 1.986(2), Li–O2 1.962(2), Li–O3 1.985(2), B–C2 1.6415(15); N1–C1–N2 102.22(9), C1–Li–O1 125.32(10), C1–Li–O2 116.28(10), C1–Li–O3 107.33(10), O1–Li–O2 96.38(9), O1–Li–O3 104.77(9), O2–Li–O3 104.56(10).

one of the signals significantly shifted to lower field because of the strong *trans*-influence of the WCA-NHC ligand. The carbene signal is found as a doublet at 153.6 ppm with $^1J(^{13}\text{C}, ^{103}\text{Rh}) = 41.9$ Hz, which is at significantly higher field in comparison with $\delta = 187.5$ ppm established for 5. Most notably, two distinctly different chemical shifts are found for the *ipso*-carbon atoms of the Dipp substituents at 134.4 ppm (sharp signal, $\nu_{1/2} = 1.4$ Hz) and at 125.5 ppm (broad signal, $\nu_{1/2} = 4.4$ Hz), suggesting the presence of an arene–rhodium interaction in solution.

The molecular structure of 4 was established by X-ray diffraction analysis (Figure 4), confirming that indeed a complex with the composition $[(\text{WCA-NHC})\text{Rh}(\text{COD})]$ had formed. The Dipp substituent adjacent to the borate moiety displays an arene–metal interaction, which involves the *ipso*-

Scheme 2. Preparation of Complex 4; Related Rhodium(I) Complexes

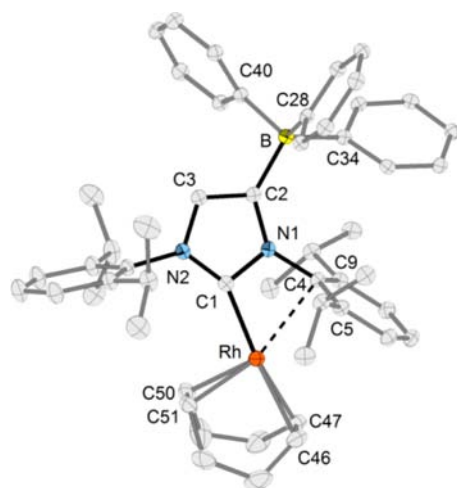
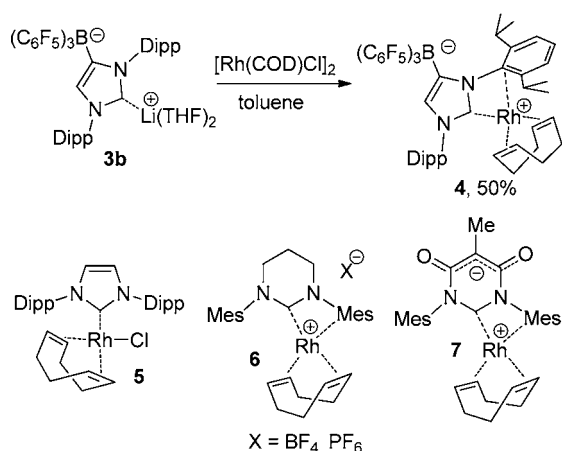


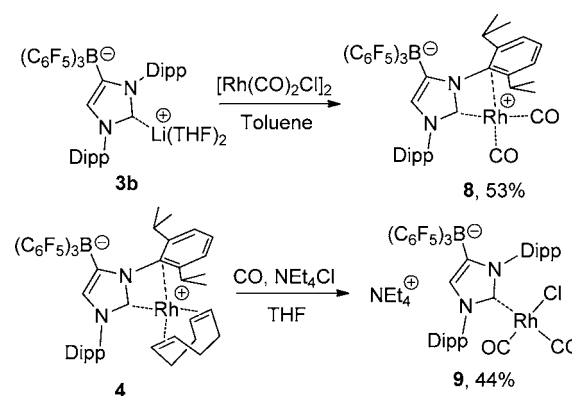
Figure 4. ORTEP diagram of **4** with thermal displacement parameters drawn at 30% probability. Hydrogen and fluorine atoms are omitted for clarity. Selected bond lengths [Å] and angles [°] (see also Table 1): Rh–C1 2.027(2), Rh–C4 2.4663(19), Rh–C5 2.6485(23), Rh–C9 3.1378(21), Rh–C46 2.227(2), Rh–C47 2.196(2), Rh–C50 2.102(2), Rh–C51 2.104(2), B–C2 1.648(3); N1–C1–N2 104.72(17), C1–N1–C4 109.78(16).

carbon atom (Rh–C4 = 2.4663(19) Å) and, possibly, one of the two *ortho*-carbon atoms (Rh–C5 = 2.6485(23) Å, Rh–C9 = 3.1378(21) Å). As a consequence, the carbene ligand is appreciably twisted to one side, which affords disparate Rh–C1–N1 and Rh–C1–N2 angles of 105.70(14)° and 149.28(15)° together with C1–N1–C4 and C2–N1–C4 angles of 109.78(16)° and 136.65(17)°. This distortion can also be described as an inclination of the Rh–C1 bond by ~23.5° to the pseudo-C2 axis defined by the carbene carbon atom C1 and the centroid of the imidazole (Ct_{Im}) plane; however, the Rh–C1 bond length of 2.027(2) Å is similar to the corresponding distance of 2.056(4) Å in **5**²⁰ and remains largely unaffected by the bending of the carbene ligand.

Similar structural motifs involving intramolecular rhodium–arene interaction had been observed previously in the solid state for the ionic complexes **6**, which contain the six-membered NHC 1,3-dimesityl-3,4,5,6-tetrahydropyrimidin-2-ylidene,²¹ and for the zwitterionic complex **7**, in which the carbene ligand contains a remote anionic functional group

within the heterocyclic backbone (Scheme 2).²² Consequently, short contacts between the metal atom and the *ipso*-carbon atoms are found, cf. Rh– C_{ipso} = 2.377(4)/2.353(5) Å in **6** (X = BF_4/PF_6) and Rh– C_{ipso} = 2.346(2) Å in **7**. In addition, complexes **6** exhibit two markedly different distances between the metal atom and the respective *ortho*-carbon atoms, cf. Rh– C_{ortho} = 2.624(5)/3.061(4) Å for X = BF_4 and Rh– C_{ortho} = 2.755(6)/2.965(6) Å for X = PF_6 ,^{21a,b} which is similar to the situation established for **5** (*vide supra*). In contrast, this disparity is less pronounced in **7** with Rh– C_{ortho} distances of 2.806(2) and 2.873(1) Å.^{22a} It is worth mentioning that for related complexes, in which the anionic carbene ligands bear fluorinated aryl substituents, no intramolecular arene–rhodium interaction could be detected experimentally.²³

As with $[\text{Rh}(\text{COD})\text{Cl}]_2$, the lithium salt **3b** reacted with $[\text{Rh}(\text{CO})_2\text{Cl}]_2$ to afford the zwitterionic dicarbonyl rhodium(I) complex **8** in 53% yield as a yellow crystalline solid (Scheme 3).

Scheme 3. Preparation of the Carbonyl Rhodium(I) Complexes **8** and **9**

The NMR chemical shifts associated with the carbene ligand are very similar to those established for the COD complex **4** (*vide supra*). Thus, the ¹³C NMR signal for the carbene carbon atom is again found at unusually high field as a doublet with δ = 154.3 ppm and $^1J(^{13}\text{C}, ^{103}\text{Rh})$ = 31.5 Hz, whereas the carbonyl carbon resonances appear as doublets at δ = 178.1 ppm with $^1J(^{13}\text{C}, ^{103}\text{Rh})$ = 100.0 Hz and at δ = 184.8 ppm with $^1J(^{13}\text{C}, ^{103}\text{Rh})$ = 56.1 Hz, whereby the latter can be assigned to the CO group in *trans*-position to the WCA-NHC ligand. The presence of a strong *trans*-effect is also reflected by the Rh–CO bond lengths determined by X-ray diffraction analysis of **8**·1/2CH₂Cl₂, with the Rh–C46 bond length of 1.8379(19) Å to the *cis*-carbonyl group being significantly shorter than the Rh–C47 bond length of 1.936(2) Å to the *trans*-carbonyl group (Figure 5). This also results in different C–O bond distances of 1.135(2) (C46–O1) and 1.124(2) Å (C47–O2), indicating that Rh–CO π -back donation is slightly stronger for the *cis*-CO group. The Rh– $\text{C}_{\text{carbene}}$ distance of 2.0133(17) Å (Rh–C1) is just slightly shorter than that in **4** (2.027(2) Å), and the arene moiety adjacent to the borate ion is also coordinated in a similar fashion to that found in **4**, albeit displaying a stronger interaction with the metal atom as indicated by consistently shorter Rh– C_{ipso} and Rh– C_{ortho} distances of 2.3988(16) (Rh–C4), 2.5823(17) (Rh–C5) and 2.9862(22) Å (Rh–C9). The bending of the carbene ligand is also similar, as indicated for instance by an inclination angle of 23.2° between the Rh–C1 and C1– Ct_{Im} axes (Table 1).

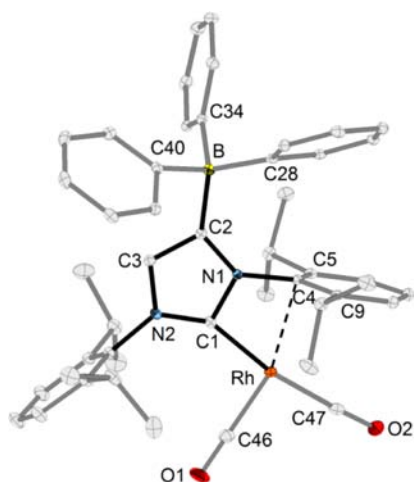
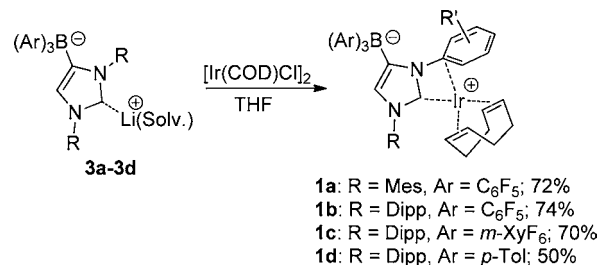


Figure 5. X-ray structure of **8** with thermal displacement parameters drawn at 30% probability. Hydrogen and fluorine atoms are omitted for clarity. Selected bond lengths [Å] and angles [°] (see also Table 1): Rh–C1 2.0133(17), Rh–C4 2.3988(16), Rh–C5 2.5823(17), Rh–C9 2.9862(22), Rh–C46 1.838(2), Rh–C47 1.936(2), C46–O1 1.135(2), C47–O2 1.124(2), B–C2 1.655(2); N1–C1–N2 105.98(14), C1–N1–C4.

In the IR spectrum of **8**, the CO stretching frequencies are found at 2100 and 2037 cm^{-1} with an average value of 2069 cm^{-1} , which is as expected significantly higher than established for neutral chloro complexes of the type [(NHC)Rh(CO)₂Cl].^{19b} Comparison of the electronic character and donor ability of the WCA-NHC ligand present in **8** with those of other NHCs required the preparation of an anionic complex [(WCA-NHC)Rh(CO)₂Cl][−], which should be accessible by reaction of **8** with a chloride source. However, we found that the preparation of such a complex was better achieved from the COD complex **4** by reaction with NEt₄Cl in THF under CO atmosphere (Scheme 3). The resulting ammonium–rhodate complex NEt₄[(WCA-NHC)Rh(CO)₂Cl] (**9**) did indeed show spectroscopic characteristics very similar to those of the corresponding neutral NHC complexes, and for instance, the ¹³C NMR resonances for the metal-bound carbon atoms are found as doublets at $\delta_{\text{carbene}} = 180.6$ ppm (¹J(¹³C,¹⁰³Rh) = 47.3 Hz) and at $\delta_{\text{CO}} = 182.9, 186.7$ ppm (¹J(¹⁰³Rh,¹³C) = 76.3, 53.2 Hz), closely resembling the values reported for [(IDipp)Rh(CO)₂Cl].²⁴ Furthermore, the CO stretching vibrations of 2067 and 1989 cm^{-1} (av. 2028 cm^{-1}) also match those measured for the neutral analog with average values of 2032^{24a} and 2037 cm^{-1} ,^{24b} indicating at best a marginal increase of the donor ability by borate substitution. Accordingly, one may conclude that, in zwitterions such as **4** and **8**, the negative charge at the borate ion is well separated from the cationic metal complex fragment and that these complexes emulate the charge distribution and reactivity of their cationic analogs,²⁵ notwithstanding their potentially quite different solubility (*vide infra*).

Synthesis and Characterization of Iridium(I) Complexes. As described for the synthesis of the rhodium(I) species **4**, the corresponding iridium(I) COD complexes of the type [(WCA-NHC)Ir(COD)] (**1**) are conveniently accessible by reaction of the lithium salts **3a–3d** with [Ir(COD)Cl]₂, although THF rather than toluene was used (Scheme 4). After stirring overnight, the solvent was removed *in vacuo* and the residues were extracted with dichloromethane, filtered through

Scheme 4. Preparation of Iridium(I) Complexes **1a–1d**



Celite, evaporated, and recrystallized from benzene to afford the complexes **1a–1d** in moderate to good yields (50–74%) as bright red or orange crystalline solids. Attempts to prepare a similar complex from **3e** (R = *t*Bu) failed, and a mixture of unidentified products was obtained instead.

The complexes **1b** and **1c** (R = Dipp; Ar = C₆F₅, *m*-XyF₆) are air-stable,²⁶ whereas **1d** (R = Dipp, Ar = *p*-Tol) is slightly air-sensitive and **1a** (R = Mes, Ar = C₆F₅) decomposes quickly even in the solid state with formation of a complex mixture of products. Similar to complex **4**, the ¹H NMR spectra of all iridium compounds show two distinct sets of signals for each aryl group and also for the CH=CH and CH₂CH₂ moieties of the COD ligand. Characteristic carbene signals are observed in the ¹³C NMR spectra in a narrow range between 149.4–151.1 ppm, which is again at significantly higher field than reported for neutral complexes of the type [(NHC)Ir(COD)Cl].^{19b,27} The olefinic carbon atoms of the COD ligand give rise to singlets at 87.0–87.5 ppm and at 52.0–52.9 ppm, with the resonances at lower field being assigned to the double bond in *trans*-position to the carbene ligand.

All four iridium complexes were additionally characterized by single-crystal X-ray diffraction, and the structure of one of the two independent molecules of **1b** is shown in Figure 6, whereas those of **1a**, **1c**, and **1d** are assembled in Figures S2–S4. For comparison, characteristic geometrical parameters of **1a–1d** are compiled in Table 1. In all cases, intramolecular coordination of the arene ring next to the borate moiety is observed, resulting

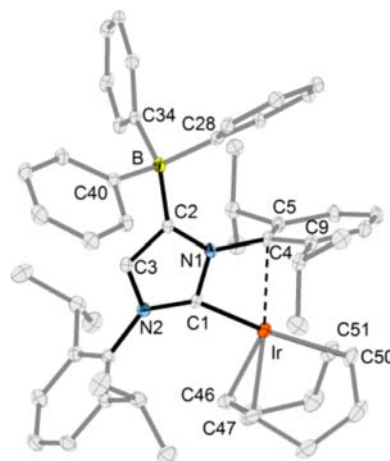


Figure 6. X-ray structure of **1b** (only one of the two independent molecules is shown) with thermal displacement parameters drawn at 30% probability. Hydrogen and fluorine atoms are omitted for clarity. Selected bond lengths [Å] and angles [°] (see also Table 1): Ir–C1 2.027(2), Ir–C4 2.447(2), Ir–C5 2.571(3), Ir–C9 3.1463(21), Ir–C46 2.099(3), Ir–C47 2.107(3), Ir–C50 2.173(3), Ir–C51 2.221(3), B–C2 1.646(4); N1–C1–N2 104.9(2), C1–N1–C4 108.1(2).

in a structural distortion and twisting of the carbene ligand in a very similar fashion to that described for the corresponding rhodium–COD complex **4** (and also for its dicarbonyl congener **8**, *vide supra*). Since the Ir–C_{carbene} distances are all very similar (Ir–C1 = 2.019(2)–2.027(2) Å) and are also virtually identical with the Rh–C_{carbene} distance in **4** (Rh–C1 = 2.027(2) Å), all distances and angles within the M–C1–N1–C4 units are very much alike, and the pronounced disparity of the metal–C_{ortho} distances (M–C5, M–C9) suggests the presence of η^2 -bound aryl groups.

It should be noted that, unlike the situation established for the rhodium complexes **5–7** (Scheme 2), we are not aware of any other iridium–carbene complexes featuring an intramolecular arene–metal interaction as present in complexes **3a–3d**. Indeed, Buchmeiser and co-workers reported the failure of all attempts to prepare a cationic iridium complex from a neutral tetrahydropyrimidin-2-ylidene complex of the type [(NHC)Ir(COD)Cl] by reaction with AgPF₆ in an analogous manner to that described for the rhodium systems **6** (Scheme 2). The ion exchange with silver(I) triflate also failed to induce arene coordination, instead affording the covalent species [(NHC)Ir(COD)(O₃SCF₃)].^{21b} Moreover, previous examples of intramolecular arene coordination involving five-membered NHC ligands are extremely rare, and we are only aware of two other complexes, namely $[(\eta^5\text{-C}_5\text{H}_5)\text{M}(\text{IMes})(\text{CO})_2][\text{B}(\text{C}_6\text{F}_5)_4]$ (M = Mo, W), for which a η^2 -coordination of one of the mesityl substituents was confirmed in the solid state.²⁸ This clearly called for a theoretical analysis of the bonding situation in our WCA–NHC rhodium and iridium complexes.

Theoretical Calculations. For transition-metal complexes of aryl-substituted N-heterocyclic carbenes, it has recently been established that, in addition to the conventional picture of metal–NHC bonding,²⁹ interaction can occur through π -face donation from the aromatic substituents and involves, in particular, the *ipso*-carbon atoms.^{30–32} Calculations revealed the operation of two different mechanisms: (1) direct donation to empty metal orbitals and (2) donation to another arene moiety that is bound to the metal atom,³¹ as evidenced, for instance, by π – π interactions between mesitylene and benzylidene groups in the solid-state structures of second-generation Grubbs-type catalysts.³³ Notably, direct donation from the C_{*ipso*} of the N-aryl group to vacant metal orbitals was held responsible for the observation that the redox potentials of several imidazolin- and imidazolidin-2-ylidene complexes of the type [(NHC)M(COD)Cl] (M = Rh,^{30d} Ir)^{30b} depend on the nature of the substituents at the *para*-position of the N-xylyl rings.³¹ It should be noted, however, that structural evidence for metal–arene interaction is not available here.

In contrast, strong arene–metal coordination is found in the rhodium complexes **4** and **8** and also in the iridium complexes **1a–1d**, involving in all cases the aryl substituents next to the borate moiety (*vide supra*). To assess the strength of this interaction, we have carried out DFT calculations on two different isomers of the complexes [(WCA–NHC)M(COD)] (M = Rh, **4**; M = Ir, **1b**), where the transition metal is bound to either one of the Dipp substituents. The standard Pople basis set 6-311G(d,p) was employed for all main group elements and a Stuttgart–Dresden basis set and effective core potential for iridium and rhodium. All calculations were carried out using the hybrid density functional B3LYP and the local meta-GGA M06L functional. Furthermore, we were able to locate the respective transition states for the interconversion of these isomers. The resulting energy profile for the iridium and

rhodium compounds is depicted in Figure 7. For both systems, the experimentally observed isomer, in which the transition

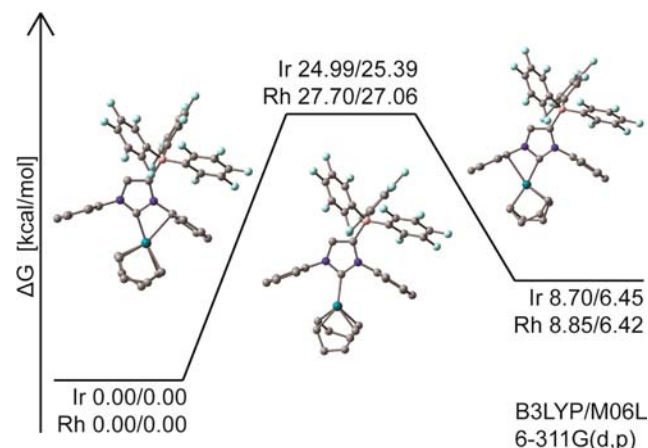
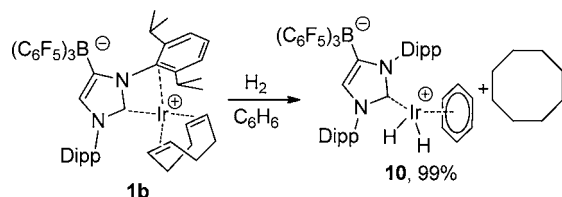


Figure 7. Calculated Gibbs free energy profile for intramolecular arene coordination in the rhodium and iridium complexes **4** and **1b** and interconversion between the experimentally observed *syn*- and hypothetical *anti*-isomers. The values indicate the energies derived with the two different density functionals B3LYP and M06L. The calculated structures of the iridium complexes are shown; for structural parameters, see Table 1 and Supporting Information.

metal is bound to the borate-flanking aryl group, is energetically favored by 6–9 kcal/mol (depending on the density functional), and the activation barrier for the interconversion is in the order of 25–28 kcal/mol.

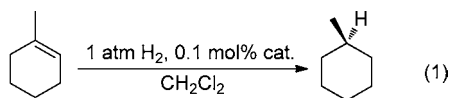
The latter values indicate that the intramolecular arene–metal interaction is strong and falls in the order of magnitude established for the bond dissociation energies of transition-metal olefin complexes.³⁴ Overall, the structural parameters calculated for the energy minima are in reasonable agreement with the solid state structures of **4** and **1b**, and the WCA–NHC–metal interaction is well reproduced, although longer metal–carbon distances are consistently predicted (Table 1). In both the experimental and the calculated molecular structures, the presence of short intramolecular C–F...C_{*ipso*} contacts in the ranges 2.721(2)–2.746(2) Å (expt) and 2.653–2.812 Å (calcd) are observed, which involve the *ortho*-fluorine atom of one C₆F₅ group and fall well below the van der Waals cutoff criterion of 3.17 Å ($r_{\text{vdW}}(\text{F}) = 1.47$ Å, $r_{\text{vdW}}(\text{C}) = 1.70$ Å).³⁵ This and other types of interaction such as π -stacking observed in **1a** (see Supporting Information) might provide an explanation for the discrimination of the two arene sites. Still, the reasons for the significantly stronger binding of the borate-flanking aryl group cannot be given at this stage and need to be investigated in more detail.

Hydrogenations. Before exploiting the iridium complexes **1a–1d** as catalysts for olefin hydrogenation, the interaction of one representative, complex **1b**, with dihydrogen was studied (Scheme 5). A suspension of **1b** in benzene-*d*₆ was stirred under atmospheric H₂ pressure for 1 h. During this time, the reaction mixture changed from intense red to colorless, and a clear solution was obtained. The ¹H NMR spectrum revealed that the signals of the COD ligand had disappeared, and a sharp singlet at 1.53 ppm was observed instead that can be assigned to the 16 H atoms of cyclooctane. In addition, a singlet at –16.21 ppm (2H) characteristic of iridium hydride species had appeared. The reaction was repeated on a larger scale (100 mg of **1b**) in benzene, and the product was isolated in pure form by

Scheme 5. Reaction of Complex **1b** with H₂ in Benzene

evaporation. The ¹H NMR spectrum of this sample showed an additional sharp singlet for coordinated benzene at 5.75 ppm, indicating that the half-sandwich dihydrido complex **10** had formed (Scheme 5). X-ray diffraction analysis confirmed the structure of **10** and the presence of an iridium(III)-bound η⁶-C₆H₆ ligand. However, the structure was very large, with two independent molecules of **10** and five noncoordinated benzenes, some of which suffered from disorder; consistent with the low quality of the structure, which we do not present in detail, the positions of the hydridic hydrogen atoms could be established only for one of the two independent molecules and then only very tentatively (Figure S5). Related cationic complexes, such as [(η⁶-C₆H₆)IrH₂(PiPr₃)]BF₄, [(η⁶-C₆H₆)IrH₂(IMes)]PF₆, and [(η⁶-Ar)IrH₂(IDipp)]BARF (Ar = C₆H₃F, C₆H₅CH₃) were reported to have similar structural and spectroscopic properties,³⁶ with the IMes complex displaying ¹H NMR signals at -15.78 and 5.93 ppm (in CD₂Cl₂) for the IrH₂ and C₆H₆ resonances, respectively.^{36b}

The formation of **10** suggests that arenes might inhibit the catalytic activity and should be avoided as solvents for hydrogenations catalyzed by complexes **1**.³⁷ In fact, neither a solution of complex **10** nor a solution of **1b** in benzene proved active in the hydrogenation of *cis*-cyclooctene (1 atm of H₂, 2 h). To benchmark the activities of the new catalysts **1**, we studied the hydrogenation of 1-methylcyclohexene at room temperature and atmospheric dihydrogen pressure in dichloromethane in the presence of catalytic amounts (0.1 mol %) of **1a–1d** (eq 1). For comparison, the traditional Crabtree's



catalyst **A** with the BARF counterion was also studied under these conditions,³⁸ and the resulting conversion–time diagrams are shown in Figure 8. For **A**, the reaction is fastest at the beginning with almost no induction period, but the reaction stops at 32% conversion after 1 h, which is in agreement with the previous findings.² A maximum turnover frequency (TOF_{max})³⁹ of 590 h⁻¹ can be determined for this system, which makes it the fastest in this comparative by study; however, its lack of stability and relatively rapid deactivation under the reaction conditions did not allow full conversion to be reached. For the WCA-NHC complexes **1a–1d**, the highest initial activity was displayed by complex **1c** (TOF_{max} = 532 h⁻¹), but its low stability resulted in the expiration of activity within 80 min with only 57.5% conversion. Complexes **1a** and **1d** were almost inactive under these reaction conditions and achieved only 12.6% and 5.6% final conversion with deactivation within ≈15 min. These findings indicate that both a weakly coordinating fluorinated borate moiety and sterically demanding Dipp substituents are required for the observation of sufficient catalytic activity. Thus, **1b** was found

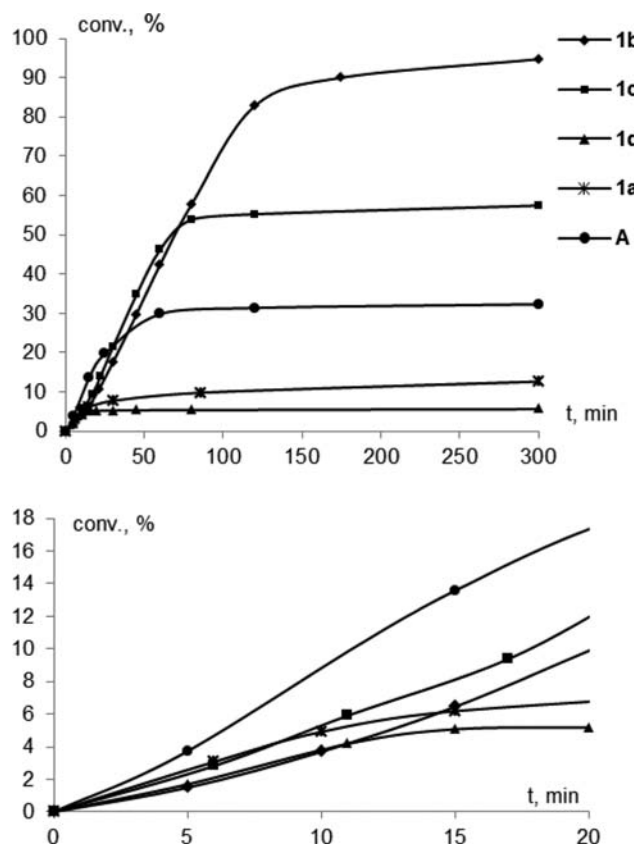


Figure 8. Catalytic performance of **1a–1d** and **A** in the hydrogenation of 1-methylcyclohexene (1 mmol) in CH₂Cl₂ (5 mL) with 0.1 mol % catalyst loading.

to be the only catalyst capable of achieving almost full conversion (95%) within 5 h with a TOF_{max} = 510 h⁻¹.

Since complex **1b** is moderately soluble in nonpolar solvents, we tested its activity by using cyclohexane as the solvent for the hydrogenation of various alkene substrates (Table 2). **1b** is

Table 2. Hydrogenation of Alkenes in Cyclohexane^a

substrate	product	cat. load, mol %	time/temp, min/°C	conv.
1-octene	1-octane	0.01	11/rt	78%
			22/rt	98%
cyclooctene	cyclooctane	0.01	22/rt	67%
			82/rt	98%
			12/rt	73%
1-methylcyclohexene	1-methylcyclohexane	0.1	27/rt	96%
			60/rt	99%
			30/rt	45%
tetramethylethylene	tetramethylethane	0.1	60/rt	62%
			30/70	98%

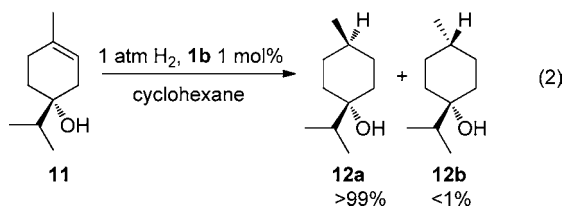
^aConditions: 1 mmol of alkene, 1 μmol or 0.1 μmol of **1b** (a stock solution in cyclohexane used), 5 mL of cyclohexane, ~1 atm of H₂.

indeed highly active in this solvent even at low catalyst loadings of 0.01 mol % toward mono- and disubstituted olefins with maximum TOFs of 42 545 h⁻¹ (for 1-octene) and 23 466 h⁻¹ (for *cis*-cyclooctene). It is worth mentioning that, in contrast to other known NHC-iridium catalysts,^{13e} no isomerization products were observed during the hydrogenation of 1-octene at low conversions and only traces (<1%) of side products were

detected by gas chromatography (GC) at higher conversions. These results demonstrate that **1b** does not act as a dehydrogenation catalyst, and this was further corroborated by heating decane and cyclooctene under reflux in the presence of **1b** (1 mol %), which did not lead to dehydrogenation.

At 0.1 mol % catalyst loading, **1b** is also able to rapidly hydrogenate the trisubstituted olefin 1-methylcyclohexene with maximum TOF of 4352 h⁻¹. Under the same conditions, hydrogenation of one of the most demanding substrates, the tetrasubstituted 2,3-dimethyl-2-butene, stopped at 62% conversion after 60 min. Nevertheless, performing the reaction at elevated temperature (70 °C) allowed a full conversion of 2,3-dimethyl-2-butene into 2,3-dimethylbutane within 30 min at 0.1 mol % catalyst loading and at 1 atm of H₂. Hydrogenation of 1-methylcyclohexene and full conversion into methylcyclohexane within 40 min was also achieved in *n*-hexane solution. It should be noted, however, that the formation of small amounts of an orange precipitate was observed at ~80% conversion, suggesting that hydrogenation proceeds partially in heterogeneously catalyzed fashion in *n*-hexane. Therefore, cyclohexane seems to be the solvent of choice.⁴⁰

High diastereoselectivity represents one of the important characteristics of Crabtree-type catalysts as a result of directing effects.⁴¹ Crabtree and co-workers reported that hydrogenation of 4-terpinenol (**11**) in CH₂Cl₂ afforded almost exclusively the isomer **12a** in >99%, and only traces of the other isomer **12b** were formed (eq 2).^{41b} In our hands and under the conditions



described by Crabtree and co-workers (despite using cyclohexane as solvent), complex **1b** gave also >99% of the stereoisomer **12a**. Upon decreasing the catalyst loading from 1 to 0.1 mol %, however, the selectivity also decreased, and a mixture of the diastereomers **12a** (98.3%) and **12b** (1.7%) was obtained.

Since the overall neutral charge of **1b** renders this complex soluble in nonpolar solvents, such as cyclohexane, we tested its applicability for catalytic hydrogenation in neat alkenes. There are only a few reports on the use of homogeneous hydrogenation catalysts in neat alkenes; however, the turnover numbers were not satisfactory or the hydrogenations were carried out under relatively harsh conditions.⁴² In an initial experiment, dihydrogen was bubbled through a solution of 0.01 mol % of **1b** (2.4 mg) in cyclooctene (2.24 g) with vigorous stirring. According to ¹H NMR data, 95% conversion to cyclooctane was achieved within 10 h with TOF_{max} = 1643 h⁻¹. In view of the low catalyst loading and the high alkene excess, the subsequent hydrogenations were performed at elevated hydrogen pressure (8 bar) by use of a Büchi “tinyclave” glass reactor. The results obtained for the hydrogenation of various neat alkenes are summarized in Table 3. Generally, disubstituted alkenes are fully hydrogenated under these conditions within a few hours at 0.01 mol % catalyst loading, and in all cases, no side products were observed by ¹H NMR spectroscopy or GC analysis (Table 3, entries 1, 2, and 5–7), whereby the hydrogenation of β-pinene afforded a mixture of

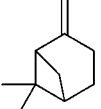
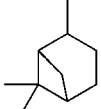
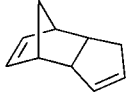
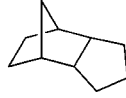
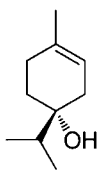
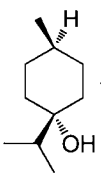
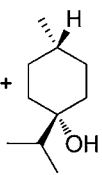
endo- and *exo*-pinane in a 1:6 ratio (entries 5 and 6). Trisubstituted 1-methylcyclohexene was fully hydrogenated within 3 h at 0.1 mol % catalyst loading (entry 8). Under the same conditions, tetrasubstituted 2,3-dimethyl-2-butene was converted into the corresponding alkane with only 41% yield (entry 9). The activity of **1b** in the hydrogenation of styrene is slightly reduced, possibly because of catalyst inhibition by arene coordination as observed for **10** (entries 10–12). Nevertheless, styrene could be completely reduced to ethylbenzene at high H₂ pressure (50 bar) and 0.01 mol % catalyst loading (entry 13). In the case of dicyclopentadiene, hydrogenation at room temperature did not result in full conversion because of solidification of the reaction mixture. The reaction was therefore carried out at 60 °C, which is beyond the melting point of the product (entry 7). Hydrogenation of 4-terpinenol (**11**) at room temperature gave 87% conversion with 97% of the directed isomer **12a** and 3% of the diastereomer **12b** with solidification of the reaction mixture (entry 14). Full conversion was achieved again at 60 °C with 96% of **12a** and 4% **12b** (Table 3, entry 15). Catalyst **1b** can also be employed for the processing of vegetable oils, and hydrogenation of rapeseed oil resulted in solidification at 47% conversion at 0.03 mol % catalyst loading as judged by ¹H NMR spectroscopy (entry 16).

Further experiments were carried out aiming at reducing the catalyst loading to 10 ppm (0.001 mol %) for the hydrogenation of *cis*-cyclooctene (Table 3, entries 3 and 4). At this concentration, the catalyst is inactive toward the crude substrate, which had just been filtered through Al₂O₃ prior to use. In contrast, *cis*-cyclooctene redistilled over KOH could be completely hydrogenated within 8 h at 20 ppm and in 12 h at 10 ppm catalyst loading at room temperature and an H₂ pressure of 8 bar. To exclude the possibility that other impurities might be catalytically active, *cis*-cyclooctene was stirred in a control experiment for 24 h under 8 bar of H₂ in the same glassware, which resulted in no conversion to cyclooctane at all, as indicated by ¹H NMR spectroscopy. Subsequent addition of **1b** to this solution gave complete hydrogenation within 12 h under the previous conditions.

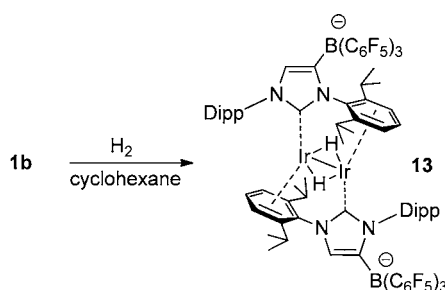
The possibility of recycling the catalyst was also investigated. Thus, the catalyst **1b** (1.2 mg, 0.1 mol %) was mixed with 1-methylcyclohexene (96 mg, 1 mmol) and dissolved in cyclohexane (total volume = 5 mL). After stirring the reaction mixture for 2 h under H₂ atmosphere (1 atm), all volatiles were evaporated and condensed into a cold trap (−196 °C, liquid N₂). GC analysis of the distillate revealed full conversion to methylcyclohexane. The same amount of the substrate solution was added, and hydrogenation was continued for another 2 h under the same conditions. GC analysis showed that only 31% conversion had been achieved, indicating that the catalytically active species undergoes partial, but relatively slow, deactivation. We observed that at high catalyst loadings (1 mol %) in cyclohexane solution, the initially red-orange reaction mixture faded by changing to orange and yellow and became almost completely colorless at ~90% conversion; this behavior is similar to that reported for NHC–phosphine iridium(I) complexes.^{13a} Finally, small amounts of a brown precipitate formed after full conversion.

To identify potential deactivation products, complex **1b** was stirred overnight under 1 atm of H₂ in cyclohexane in the absence of any substrate, and a brown microcrystalline precipitate was isolated by filtration (Scheme 6). The resulting solid is only slightly soluble in dichloromethane and acetone. Its ¹H NMR spectrum (in acetone-*d*₆) indicated the presence of

Table 3. Hydrogenation in Neat Alkenes

Entry	Substrate	Product	Cat. loading, H ₂ pressure	Time	Conversion, % ^a
1			0.01 mol%, 1 bar	10 h	95
2			0.01 mol%, 8 bar	1 h	100
3 ^b	cyclooctene	cyclooctane	0.002 mol%, 8 bar	8 h	100
4 ^b			0.001 mol%, 8 bar	12 h	100
5			0.01 mol%, 8 bar	2 h	44
6			0.01 mol%, 8 bar	13 h	100
7 ^c			0.01 mol%, 8 bar	2 h	100
8	1-methylcyclohexene	1-methylcyclohexane	0.1 mol%, 8 bar	2 h	100
9	tetramethylethylene	tetramethylethane	0.1 mol%, 8 bar	2 h	41
10			0.1 mol%, 8 bar	2 h	100
11	styrene	ethylbenzene	0.01 mol%, 8 bar	2 h	9
12			0.01 mol%, 8 bar	13 h	41
13			0.01 mol%, 50 bar	4 h	100
14			0.1 mol%, 8 bar	2 h	87 (97:3)
15 ^c				2 h	100 (96:4)
16	rapeseed oil	saturated fat	0.03 mol%, 8 bar	3 h	47 (solid)

^aAccording to NMR and GC data. ^bRedistilled alkene was used. ^cReaction was carried out at 60 °C.

Scheme 6. Reaction of 1b with H₂ in Cyclohexane

two different ligand fragments along with a characteristic high-field resonance at -15.81 ppm that can be assigned to one Ir–H moiety per WCA-NHC ligand by integration.⁴³ The ¹¹B NMR spectrum exhibits two close signals with the same intensity at -13.8 and -14.2 ppm. High-resolution ESI-MS showed the most salient peak at $m/z = 2185.4743$ (calculated: 2185.4748), which corresponds to the binuclear complex [(WCA-NHC)₂Ir₂H₂] (13). This composition was confirmed by elemental analysis for 13·C₈H₁₆ with a tightly bound cyclooctane molecule that could not be removed even by prolonged drying under high vacuum. The compound is inert toward alkenes, as demonstrated by treatment with cyclooctene in refluxing cyclohexane, and it is insoluble in benzene.

Therefore, 13 can be regarded as the main deactivation product, if hydrogenation is performed in cyclohexene under 1 atm of H₂. Two types of single crystals, orange needles and red prisms, were grown from a saturated solution of 13 in acetone, and X-ray diffraction analyses revealed for both cases the presence of the binuclear complex 13. Since the structure of the red modification suffered from severe disorder, even of the iridium atoms, we do not present it here. Unfortunately, the position of the hydridic hydrogen atoms could not be determined for the orange modification, but the Ir–Ir distance of 2.6539(4) Å indicates a metal–metal bond, which falls in the range observed for related complexes featuring an Ir₂H₂ moiety with bridging hydrogen atoms (Figure 9).⁴⁴

The WCA-NHC ligands are coordinating the two Ir atoms in a $\mu-\eta^1:\eta^6$ fashion with Ir–C_{carbene} bond lengths of Ir1–C1 = 2.052(7) Å and Ir2–C46 = 2.061(7) Å. This bridging mode was previously observed in complexes containing aryl-substituted NHCs^{36c,45} and phosphines.⁴⁶ Surprisingly, a tetrahydride structure with a [IrH(μ -H)]₂ core was assigned to the structurally most closely related compound, [(IDipp)₂Ir₂H₄][BARF]₂, which gives rise to a hydride resonance at $\delta = -15.73$ ppm. It should be noted, however, that the reported crystal structure also suffers from serious disorder.^{36c} Surprisingly, a disparate arene coordination mode is observed for the two carbene ligands: The carbene at Ir1 binds

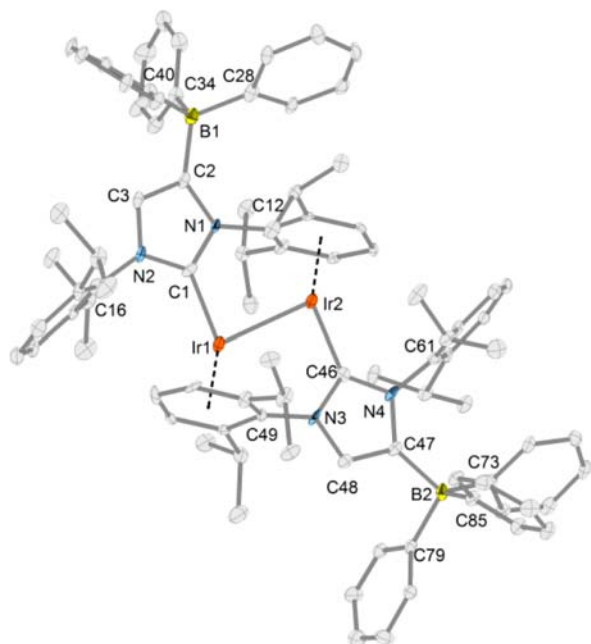


Figure 9. X-ray structure of **13** with thermal displacement parameters drawn at 30% probability. Hydrogen and fluorine atoms are omitted for clarity. Selected bond lengths [Å] and angles [°]: Ir1–C1 2.052(7), Ir2–C46 2.061(7), Ir1–Ir2 2.6539(4), Ir1–C_{arene} 2.183(7)–2.433(8), Ir2–C_{arene} 2.194(7)–2.389(8); C1–Ir1–Ir2 86.5(2), C46–Ir2–Ir1 87.9(2).

to Ir2 via the Dipp substituent next to the borate group, whereas the carbene at Ir2 binds unexpectedly to Ir1 via the opposite Dipp substituent; the same was established for the red modification despite the poor quality of the structure. The reasons for this behavior remain unclear at this stage and will be further explored; however, the isolation and characterization of **13** offer a possible explanation for the deactivation processes operating for this new class of iridium-based hydrogenation catalysts in nonpolar media. In contrast, leaving a dichloromethane solution of **1b** under 1 atm of H₂ overnight led to precipitation of iridium black with formation of a complex mixture of products, from which only small amounts of **13** could be isolated.

CONCLUSION

A convenient protocol for the preparation of various lithium complexes of N-heterocyclic carbenes with a weakly coordinating borate moiety (WCA-NHC) was introduced. These lithium salts serve as valuable precursors for the synthesis of transition-metal complexes by transmetalation reactions, as demonstrated by the reaction with [M(COD)Cl]₂ to afford the zwitterionic complexes [(WCA-NHC)M(COD)] (M = Rh, Ir). In the solid state, all molecular structures exhibit carbene ligands, which are additionally bound to the metal atom through the borate-flanking aryl group, providing an exceptionally large number of experimentally confirmed examples of π -face donation in metal complexes of aryl-substituted NHC ligands.³¹ The iridium(I) complexes [(WCA-NHC)Ir(COD)] can be regarded as carbene analogues of Crabtree's catalyst [Ir(COD)(py)(PCy₃)] [PF₆] (**A**), with their overall neutral charge allowing olefin hydrogenations in nonpolar media. Complex **1b**, in which the WCA-NHC ligand bears a B(C₆F₅)₃ moiety and Dipp substituents, proved particularly active even for the hydrogenation of hindered alkenes in nonpolar solvents or of

neat alkenes. Neat hydrogenation of alkenes could be performed with catalyst loadings as low as 10 ppm at 8 atm of dihydrogen, demonstrating the marked ability of the ancillary WCA-NHC ligand to support and stabilize electrophilic transition-metal complex fragments.

ASSOCIATED CONTENT

Supporting Information

Supplementary data containing full experimental details and X-ray diffraction data. This material is available free of charge via the Internet at <http://pubs.acs.org>.

AUTHOR INFORMATION

Corresponding Author

m.tamm@tu-bs.de

Notes

The authors declare no competing financial interest.

ACKNOWLEDGMENTS

This work was supported by the Deutsche Forschungsgemeinschaft through grant TA 189/9-1. We thank Dr. Ingo Kurz and Dr. Ulrich Papke (TU Braunschweig) for their substantial support with the GC and mass spectrometric studies.

REFERENCES

- (1) (a) Crabtree, R. H.; Morris, G. E. *J. Organomet. Chem.* **1977**, *135*, 395. (b) Crabtree, R. H.; Felkin, H.; Morris, G. E. *J. Organomet. Chem.* **1977**, *141*, 205.
- (2) Crabtree, R. *Acc. Chem. Res.* **1979**, *12*, 331. *N-Heterocyclic Carbenes in Synthesis*, 1st ed.; Nolan, S. P., Ed.; Wiley-VCH: Weinheim, Germany, 2006, Chapter 10.
- (3) Helmchen, G.; Pfaltz, A. *Acc. Chem. Res.* **2000**, *33*, 336.
- (4) (a) Lightfoot, A.; Schnider, P.; Pfaltz, A. *Angew. Chem., Int. Ed.* **1998**, *37*, 2897. (b) Smidt, S. P.; Zimmermann, N.; Studer, M.; Pfaltz, A. *Chem.—Eur. J.* **2004**, *10*, 4685. (c) Wüstenberg, B.; Pfaltz, A. *Adv. Synth. Catal.* **2008**, *350*, 174.
- (5) (a) Cipot, J.; McDonald, R.; Stradiotto, M. *Chem. Commun.* **2005**, *0*, 4932. (b) Cipot, J.; McDonald, R.; Ferguson, M. J.; Schatte, G.; Stradiotto, M. *Organometallics* **2007**, *26*, 594.
- (6) Franzke, A.; Pfaltz, A. *Chem.—Eur. J.* **2011**, *17*, 4131.
- (7) For a review on zwitterionic platinum group metal complexes see: Stradiotto, M.; Hesp, K. D.; Lundgren, R. *J. Angew. Chem., Int. Ed.* **2010**, *49*, 494.
- (8) Crabtree and co-workers reported that [Ir(COD)(py)(PCy₃)] [PF₆] is inactive in hydrogenation of alkenes in benzene, toluene, and hexane, see ref 2. Pfaltz and co-workers mentioned significantly reduced activity of phosphinooxazoline complexes of type **B** in toluene, see ref 4b.
- (9) Lee, H. M.; Jiang, T.; Stevens, E. D.; Nolan, S. P. *Organometallics* **2001**, *20*, 1255.
- (10) (a) Arduengo, A. J.; Harlow, R. L.; Kline, M. *J. Am. Chem. Soc.* **1991**, *113*, 361. (b) *N-Heterocyclic Carbenes in Synthesis*, 1st ed.; Nolan, S. P., Ed.; Wiley-VCH: Weinheim, Germany, 2006. (c) *N-Heterocyclic Carbenes in Transition Metal Catalysis*; Glorius, F., Ed.; Springer-Verlag: Berlin, Germany, 2007; (d) *N-Heterocyclic Carbenes: From Laboratory Curiosities to Efficient Synthetic Tools*; Diez-Gonzalez, S., Ed.; Royal Society of Chemistry: Cambridge, U.K., 2011.
- (11) Powell, M. T.; Hou, D.-R.; Perry, M. C.; Cui, X.; Burgess, K. *J. Am. Chem. Soc.* **2001**, *123*, 8878.
- (12) (a) Perry, M. C.; Cui, X.; Powell, M. T.; Hou, D.-R.; Reibenspies, J. H.; Burgess, K. *J. Am. Chem. Soc.* **2003**, *125*, 113. (b) Cui, X.; Burgess, K. *J. Am. Chem. Soc.* **2003**, *125*, 14212. (c) Cui, X.; Fan, Y.; Hall, M. B.; Burgess, K. *Chem.—Eur. J.* **2005**, *11*, 6859. (d) Nanchen, S.; Pfaltz, A. *Chem.—Eur. J.* **2006**, *12*, 4550. (e) Messerle, B. A.; Page, M. J.; Turner, P. *Dalton Trans.* **2006**, 3927. (f) Chen, D.; Banphavichit, V.; Reibenspies, J.; Burgess, K.

- Organometallics* **2007**, *26*, 855. (g) Kownacki, I.; Kubicki, M.; Szubert, K.; Marciniak, B. *J. Organomet. Chem.* **2008**, *693*, 321. (h) Zhao, J.; Burgess, K. *Org. Lett.* **2009**, *11*, 2053. (i) Jeletic, M. S.; Jan, M. T.; Ghiviriga, I.; Abboud, K. A.; Veige, A. S. *Dalton Trans.* **2009**, 2764. (j) Binobaid, A.; Iglesias, M.; Beetstra, D. J.; Kariuki, B.; Derivisi, A.; Fallis, I. A.; Cavell, K. J. *Dalton Trans.* **2009**, 7099. (k) Schumacher, A.; Bernasconi, M.; Pfaltz, A. *Angew. Chem., Int. Ed.* **2013**, *52*, 7422.
- (13) (a) Vazquez-Serrano, L. D.; Owens, B. T.; Buriak, J. M. *Chem. Commun.* **2002**, 2518. (b) Bolm, C.; Focken, T.; Raabe, G. *Tetrahedron: Asymmetry* **2003**, *14*, 1733. (c) Focken, T.; Raabe, G.; Bolm, C. *Tetrahedron: Asymmetry* **2004**, *15*, 1693. (d) Hodgson, R.; Douthwaite, R. E. *J. Organomet. Chem.* **2005**, *690*, 5822. (e) Vazquez-Serrano, L. D.; Owens, B. T.; Buriak, J. M. *Inorg. Chim. Acta* **2006**, *359*, 2786. (f) Nanchen, S.; Pfaltz, A. *Helv. Chim. Acta* **2006**, *89*, 1559. (g) Passays, J.; Ayad, T.; Ratovelomanana-Vidal, V.; Gaumont, A.-C.; Jubault, P.; Leclerc, E. *Tetrahedron: Asymmetry* **2011**, *22*, 562. (h) Bennie, L. S.; Fraser, C. J.; Irvine, S.; Kerr, W. J.; Andersson, S.; Nilsson, G. N. *Chem. Commun.* **2011**, 47, 11653.
- (14) Kronig, S.; Theuergarten, E.; Daniliuc, C. G.; Jones, P. G.; Tamm, M. *Angew. Chem., Int. Ed.* **2012**, *51*, 3240.
- (15) (a) Holschumacher, D.; Bannenberg, T.; Hrib, C. G.; Jones, P. G.; Tamm, M. *Angew. Chem., Int. Ed.* **2008**, *47*, 7428. (b) Holschumacher, D.; Taouss, C.; Bannenberg, T.; Hrib, C. G.; Daniliuc, C. G.; Jones, P. G.; Tamm, M. *Dalton Trans.* **2009**, 6927. (c) Holschumacher, D.; Bannenberg, T.; Ibrom, K.; Daniliuc, C. G.; Jones, P. G.; Tamm, M. *Dalton Trans.* **2010**, *39*, 10590. (d) Holschumacher, D.; Daniliuc, C. G.; Jones, P. G.; Tamm, M. *Z. Naturforsch.* **2011**, *66b*, 371. (e) Kronig, S.; Theuergarten, E.; Holschumacher, D.; Bannenberg, T.; Daniliuc, C. G.; Jones, P. G.; Tamm, M. *Inorg. Chem.* **2011**, *50*, 7344. (f) Kolychev, E. L.; Bannenberg, T.; Freytag, M.; Daniliuc, C. G.; Jones, P. G.; Tamm, M. *Chem.—Eur. J.* **2012**, *52*, 16938.
- (16) Kolychev, E. L.; Theuergarten, E.; Tamm, M. *Top. Curr. Chem.* **2013**, *334*, 121.
- (17) Wang, Y.; Xie, Y.; Abraham, M. Y.; Wei, P.; Schaefer, H. F.; Schleyer, P. v. R.; Robinson, G. H. *J. Am. Chem. Soc.* **2010**, *132*, 14370.
- (18) Arduengo, A. J., III; Krafczyk, R.; Schmutzler, R. *Tetrahedron* **1999**, *55*, 14523.
- (19) (a) Tolman, C. A. *Chem. Rev.* **1977**, *77*, 313. (b) Dröge, T.; Glorius, F. *Angew. Chem., Int. Ed.* **2010**, *49*, 6940.
- (20) Lee, S. I.; Park, S. Y.; Park, J. H.; Jung, I. G.; Choi, S. Y.; Chung, Y. K.; Lee, B. Y. *J. Org. Chem.* **2006**, *71*, 91.
- (21) (a) Imlinger, N.; Wurst, K.; Buchmeiser, M. R. *J. Organomet. Chem.* **2005**, *690*, 4433. (b) Zhang, Y.; Wang, D.; Wurst, K.; Buchmeiser, M. R. *J. Organomet. Chem.* **2005**, *690*, 5728 for X = PF₆, two independent molecules are found in the asymmetric unit with similar structural parameters..
- (22) (a) César, V.; Lugan, N.; Lavigne, G. *J. Am. Chem. Soc.* **2008**, *130*, 11286. (b) César, V.; Lugan, N.; Lavigne, G. *Chem.—Eur. J.* **2010**, *16*, 11432.
- (23) Hobbs, M. G.; Knapp, C. J.; Welsh, P. T.; Borau-Garcia, J.; Ziegler, T.; Roesler, R. *Chem.—Eur. J.* **2010**, *16*, 14520.
- (24) (a) Yu, X.-Y.; Sun, H.; Patrick, B. O.; James, B. R. *Eur. J. Inorg. Chem.* **2009**, 2009, 1752. (b) Sato, T.; Hirose, Y.; Yoshioka, D.; Oi, S. *Organometallics* **2012**, *31*, 6995.
- (25) For a thorough study of this phenomenon see: Bendeif, E.-E.; Matta, C. F.; Stradiotto, M.; Fertey, P.; Lecomte, C. *Inorg. Chem.* **2012**, *51*, 3754.
- (26) NMR analysis of a sample of **1b** obtained by evaporation of its solution under aerobic conditions gave no indication of decomposition after storage for three months in air. Stock solutions of **1b** prepared in air displayed no decrease in catalytic activity.
- (27) Kelley, R. A., III; Clavier, H.; Giudice, S.; Scott, N. M.; Stevens, E. D.; Bordner, J.; Samardjiev, I.; Hoff, C. D.; Cavallo, L.; Nolan, S. P. *Organometallics* **2008**, *27*, 202.
- (28) (a) Dioumaev, V. K.; Szalda, D. J.; Hanson, J.; Franz, J. A.; Bullock, R. M. *Chem. Commun.* **2003**, 1670. (b) Wu, F.; Dioumaev, V. K.; Szalda, D. J.; Hanson, J.; Bullock, R. M. *Organometallics* **2007**, *26*, 5079.
- (29) Jacobsen, H.; Correa, A.; Poater, A.; Costabile, C.; Cavallo, L. *Coord. Chem. Rev.* **2009**, *253*, 687.
- (30) (a) Süßner, M.; Plenio, H. *Chem. Commun.* **2005**, 5417. (b) Leuthäuser, S.; Schwarz, D.; Plenio, H. *Chem.—Eur. J.* **2007**, *13*, 7195. (c) Leuthäuser, S.; Schmidts, V.; Thiele, C. M.; Plenio, H. *Chem.—Eur. J.* **2008**, *14*, 5465. (d) Wolf, S.; Plenio, H. *J. Organomet. Chem.* **2009**, *694*, 1487.
- (31) Credendino, R.; Falivene, L.; Cavallo, L. *J. Am. Chem. Soc.* **2012**, *134*, 8127.
- (32) Fernández, I.; Lugan, N.; Lavigne, G. *Organometallics* **2012**, *31*, 1155.
- (33) Fürstner, A.; Ackermann, L.; Gabor, B.; Goddard, R.; Lehmann, C. W.; Mynott, R.; Stelzer, F.; Thiel, O. R. *Chem.—Eur. J.* **2001**, *7*, 3236.
- (34) (a) Hyla-Kryspin, I.; Srimme, S. *Organometallics* **2004**, *23*, 5581. (b) Cramer, R. *J. Am. Chem. Soc.* **1967**, *89*, 5377.
- (35) (a) Bondi, A. *J. Phys. Chem.* **1964**, *68*, 441. (b) Rowland, R. S.; Taylor, R. *J. Phys. Chem.* **1996**, *100*, 7384.
- (36) (a) Torres, F.; Sola, E.; Martín, M.; López, J. A.; Lahoz, F. J.; Oro, L. A. *J. Am. Chem. Soc.* **1999**, *121*, 10632. (b) Torres, O.; Martín, M.; Sola, E. *Organometallics* **2009**, *28*, 863. (c) Tang, C. Y.; Lednik, J.; Vidovic, D.; Thompson, A. L.; Aldridge, S. *Chem. Commun.* **2011**, 47, 2523.
- (37) For the inhibiting influence of aromatic solvents on the activity of hydrogenations, see for instance: Heller, D.; Drexler, H.-J.; Spannberg, A.; Heller, B.; You, J.; Baumann, W. *Angew. Chem., Int. Ed.* **2002**, *41*, 777.
- (38) A was prepared according to published procedures, see ref 4c. In addition, we established its X-ray crystal structure (see Supporting Information for a presentation).
- (39) TOF_{max} was determined at the steepest slope of the curve in the conversion-time diagram; see: Kozuch, S.; Martin, J. M. L. *ACS Catalysis* **2012**, *2*, 2787.
- (40) It should be noted that addition of metallic mercury did not affect the catalytic activity in the hydrogenation of 1-methylcyclohexene in cyclohexane solution at 0.1 mol% catalyst loading, therefore excluding the formation of catalytically active metallic Ir.
- (41) (a) Crabtree, R. H.; Davis, M. W. *Organometallics* **1983**, *2*, 681. (b) Crabtree, R. H.; Davis, M. W. *J. Org. Chem.* **1986**, *51*, 2655. (c) Brown, J. M. *Angew. Chem., Int. Ed.* **1987**, *26*, 190.
- (42) (a) Blum, Y.; Czarkie, D.; Rahamim, Y.; Shvo, Y. *Organometallics* **1985**, *4*, 1459. (b) Budzelaar, P. H. M.; Moonen, N. N. P.; de Gelder, R.; Smits, Jan M. M.; Gal, A. W. *Eur. J. Inorg. Chem.* **2000**, 2000, 753.
- (43) To exclude inaccurate integration because of long relaxation times, the ¹H NMR spectrum was recorded on a Bruker AV II 600 device with delay times (D1) of 15 s.
- (44) (a) Oro, L. A.; Carmona, D.; Puebla, M. P.; Lamata, M. P.; Foces-Foces, C.; Cano, F. H. *Inorg. Chim. Acta* **1986**, *112*, L11. (b) Dobbs, D. A.; Bergman, R. G. *J. Am. Chem. Soc.* **1993**, *115*, 3836. (c) Dobbs, D. A.; Bergman, R. G. *Organometallics* **1994**, *13*, 4594. (d) Hou, Z.; Fujita, A.; Koizumi, T.-a.; Yamazaki, H.; Wakatsuki, Y. *Organometallics* **1999**, *18*, 1979. (e) Fujita, K.-i.; Hamada, T.; Yamaguchi, R. *J. Chem. Soc., Dalton Trans.* **2000**, 1931. (f) Fujita, K.-i.; Nakaguma, H.; Hanasaka, F.; Yamaguchi, R. *Organometallics* **2002**, *21*, 3749. (g) Hanasaka, F.; Fujita, K.-i.; Yamaguchi, R. *Organometallics* **2005**, *24*, 3422. (h) Thewissen, S.; Reijnders, M. D. M.; Smits, J. M. M.; de Bruin, B. *Organometallics* **2005**, *24*, 5964. (i) Takahashi, Y.; Nonogawa, M.; Fujita, K.-i.; Yamaguchi, R. *Dalton Trans.* **2008**, 3546. (j) Meredith, J. M.; Goldberg, K. I.; Kaminsky, W.; Heinekey, D. M. *Organometallics* **2009**, *28*, 3546. (k) McBee, J. L.; Tilley, T. D. *Organometallics* **2009**, *28*, 5072. (l) Royer, A. M.; Rauchfuss, T. B.; Gray, D. L. *Organometallics* **2010**, *29*, 6763.
- (45) Lee, C. H.; Laiter, D. S.; Mueller, P.; Sadighi, J. P. *J. Am. Chem. Soc.* **2007**, *129*, 13802.
- (46) See examples of such coordination for rhodium: (a) Singewald, E. T.; Mirkin, C. A.; Stern, C. L. *Angew. Chem., Int. Ed. Engl.* **1995**, *34*, 1624. (b) Rifat, A.; Patmore, N. J.; Mahon, M. F.; Weller, A. S. *Organometallics* **2002**, *21*, 2856. (c) Yu, X.-Y.; Maekawa, M.; Morita, T.; Chang, H.-C.; Kitagawa, S.; Jin, G.-X. *Bull. Chem. Soc. Jpn.* **2002**,

75, 267. (d) Marcazzan, P.; Ezhova, M. B.; Patrick, B. O.; James, B. R. *C. R. Chim.* **2002**, *5*, 373. (e) Montag, M.; Leitus, G.; Shimon, L. J. W.; Ben-David, Y.; Milstein, D. *Chem.—Eur. J.* **2007**, *13*, 9043. (f) Preetz, A.; Baumann, W.; Fischer, C.; Drexler, H.-J.; Schmidt, T.; Thede, R.; Heller, D. *Organometallics* **2009**, *28*, 3673. (g) Preetz, A.; Fischer, C.; Kohrt, C.; Drexler, H.-J.; Baumann, W.; Heller, D. *Organometallics* **2011**, *30*, 5155.